



24th ABCM International Congress of Mechanical Engineering  
December 3-8, 2017, Curitiba, PR, Brazil

## COBEM-2017-2807

# NUMERICAL PROCEDURE BASED ON FINITE ELEMENTS METHOD AND THEORY OF COSSERAT RODS FOR STRUCTURES SUBJECTED TO STATIC LOADS

**Rodrigo Guilherme Baptista**

**Tháisa Silvestre**

**Marcos Hiroshi Takahama**

**Adailton Silva Borges**

Federal University of Technology - Paraná, Department of Mechanical Engineering, Alberto Carazzai Avenue, 1640, CEP:86300-000, Cornélio Procópio, Brazil

rodrigo\_gbap@hotmail.com

thaisasilvestre@hotmail.com

mhtakahama@hotmail.com

adailton@utfpr.edu.br

**Abstract:** *The present work aims to validate a numerical methodology that evaluates the displacement profile in beams subjected to static loads. This the nonlinear numerical finite element method and the Theory of Cosserat rod are the bases of the procedure. The main advantage of using the Cosserat theory is that it is geometrically accurate, which assists in the discretization of the equations of motion and the form functions are obtained from differential equations of static equilibrium, a determinant factor to consider all nonlinearities of the system. Thus, the accuracy of response is achieved more quickly, and the structure can be divided into a few elements, the number of which is much lower than a traditional analysis in which interpolation functions are often simpler as low order polynomials. For the validation, two cases were found in the literature and the results obtained by the respective authors were compared with the results achieved by the proposed methodology.*

**Keywords:** *Finite Elements, Theory of Cosserat Rods, Static Loads.*

## 1. INTRODUCTION

As the world progresses in a progressive technological evolution, the improvement and development of techniques in numerous areas of engineering are more and more constant. A branch that has been raising increasing development involves the application of numerical procedures for the analysis of structures. One of these appliances to determine the tensile and deformation states in structures is the Finite Element Method (FEM).

The aerospace industry developed the FEM in the 1950s. The main ones involved were Boeing, the long-extinct Aerospace Bell in the United States and Rolls Royce in the United Kingdom. Millions of engineers and scientists worldwide use FEM to predict structural, mechanical, thermal, electrical and chemical behavior of systems, both in the design stage and in the performance analysis (Fish, 2009). The FEM provides a systematic methodology with which the solution can be determined through a computer program and provides computational simulations that facilitate the study of structures. Instead of making the construction of several prototypes and models until the definition of the most appropriate structurally and visually (design), by the computer it occurs the easy modification of the component aiming its optimization. In addition, manufacturers increasingly want to optimize their machines by providing more safety, comfort and performance, so Finite Element (FE) analysis presents flexibility and continuous optimization is performed quicker.

Elements of beam and shell constitute a group of elements very useful in computational programs in finite elements. Traditionally the modeling of a structure bases on its geometry, in function of the specific hypotheses adopted. The most common structural types are flexible cables, bars, beams, thin or thick flat plates, cylindrical or spherical shells and compact solids (Bathe, 1996). Many of the above are slender structures and the case worked in this work will cover

this type of structure. By definition, a slender structure, for example, a beam is basically considered a curve in space and has a small cross-section compared to its length.

In addition to the geometry of the considered structure, the modeling also requires a characterization of the behavior regarding the applied forces and the deformation exhibited in the same. In this meaning, in the structural scope, two behaviors can be identified: linear and non-linear.

The linear behavior is simpler, and its main characteristic is the proportionality between applied loads and displacements and deformations of the structure, also finding that the deformation does not change the form of application of the load. The occurrence of small deformations, rotations and displacements, in the domain of which the law of Hooke prevails condition these characteristics. On the other hand, nonlinear behavior can occur in three ways: physical nonlinearity, geometric nonlinearity, and physical and geometric nonlinearity (Bathe, 1996).

Physical nonlinearity occurs when there is no proportionality between the stresses applied and the deformations resulting from an intrinsic characteristic of the material composing the structure. Some materials such as aluminum and low carbon steel, when subjected to larger deformations, exhibit non-linear behavior while for small deformations, linear behavior. The main characteristic of this nonlinearity is the occurrence of small displacements and large deformations. Geometric nonlinearity occurs when the displacements and rotations suffered by the structure influence the way in which the loads are applied and in the deformations, characterizing the occurrence of large displacements and rotations and small deformations. Physical and geometric non-linearity is a mixture of the two previously discussed and characterizes the presence of large displacements, rotations and deformations.

It is then necessary to make the appropriate choice of the underlying theory to the modeling procedures that take into account the considerations of the studied structure geometry and the profile of submitted forces and displacements obtained. Among the several studied that can be used in beams subjected to non-linearity, the theory of Cosserat rods is highlighted.

The theory of Cosserat rods was developed by the brothers Eugene and Francois Cosserat in 1909, and over the years, due to the absence or non-existence of computational tools capable of solving the nonlinear equations inherent to this theory, this one was not widely used. Already the expressive increase of computational capacity and the interest of the academic community regarding the studies of nonlinear systems explains the recent resumption of this theory.

This theory requires a high computational cost, a fact that has resulted in the use of alternative techniques of simplified modeling. However, with the recent advances obtained, both in numerical methodologies and in increasing computational capacity, this has become feasible to study problems of growing complexity.

One of the reasons for using this theory is that it is geometrically exact, that means, it is not based on geometric approximations or mechanical assumptions. The deformed beam behaves as a displacement vector of the centroid curve of the cross-sections and the orientation of a given moving base relative to an inertial reference system, which describe bending, twisting, extension and shear. Three consecutive elementary rotations parametrizes the beam (Borges, 2010).

The simple description, using the Cosserat continuum of slender structures, provides a clear delineation between basic physical principles, material properties and mathematical approximations. This method becomes feasible in problems by which linear methods are inappropriate (non-linear boundary conditions, non-linear material, complex geometry, impact, precession, internal interaction, etc.).

The main advantage of using this together with finite element analysis is that the shape functions are obtained from differential equations of static equilibrium, a determinant factor to consider all nonlinearities of the system. Thus, the accuracy of the response is reached quicker, and the structure can be divided into a few elements, the number of which is much lower than a traditional analysis in which interpolation functions are often simpler as low order polynomials.

From the union of the finite element method with the Cosserat beam theory, a numerical procedure developed in Matlab® capable of generating the displacement profile in slender structures subjected to static stresses is proposed. For the purpose of validation of this, at the end of the present work, the numerical results obtained from the methodology proposed will be compared to the results of two studies found in the literature.

## 2. THEORY OF COSSERAT RODS

The Cosserat beam theory stipulates that the behavior of a slender structure is modeled in terms of the motion in space. The line passes through the centroids of its cross sections, and the positions are defined by the vector  $r(s)$  on the Cartesian basis  $F(e_1, e_2, e_3) \equiv F$  with unit vectors  $(e_i)$  and by a set of unitary orthogonal vectors attached to the cross section  $\{d_1(s), d_2(s), d_3(s)\}$ . The mobile base  $(S)$  is defined along the centroid curve, formed by the directing vectors  $di(s)$ , where  $s$  is the distance along the line of centroids of the non-deformed beam. Note that there is an association of the directors at each point of the centroid curve. Figure 1 illustrates these notions.

It is assumed that  $d_1(s)$  and  $d_2(s)$  are contained in the cross-sectional plane, and hence  $d_3(s)$  is perpendicular to this plane. Therefore, for each point of the centroid curve there is a moving base  $s$ , formed by the unit vectors  $di(s, t)$ , which are defined externally to the vector  $r(s, t)$ . There is a classification with respect to deformation referring to the theory of cosserat rods, these are the linear deformations  $v(s)$  and the angular deformations  $u(s)$ . The components  $v_1(s)$  and  $v_2(s)$  are called shear deformations and  $v_3(s)$  elongation deformations.  $u_1(s)$  and  $u_2(s)$  are described as bending deformations and  $u_3(s)$  is called torsional deformation. To provide a complete description, it is important to establish the relationship between the linear and angular deformation to which a Cosserat beam segment is subjected, and the fixed and mobile bases, i.e. the spatial position of the centroids as well as how the rotation of the transversal section.

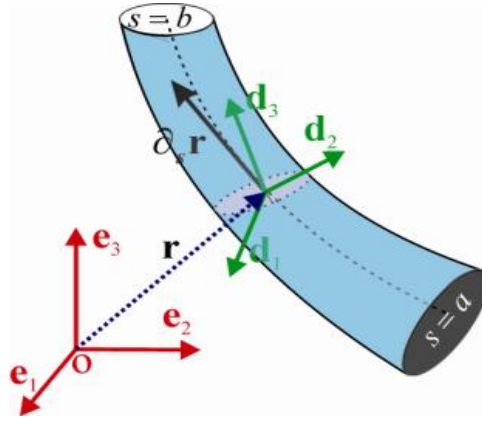


Figure 1. Schematic model of a Cosserat beam element

The vector of linear deformation  $v(s)$  is obtained from the variation of the line of centroids along the coordinate  $s$  and observed in Eq.(1):

$$F_{v(s)} = \frac{d^F r(s)}{ds} = |r'(s)|^F d_3(s) \quad (1)$$

The angular deformation vector  $u(s)$  is obtained by deriving the mobile base  $d_i(s)$  from the space as observed in Eq.(2).

$$\frac{dd_i(s)}{ds} = u(s, t) \times d_i(s, t) \quad (2)$$

From this, two parametrization methods are employed to describe the relationships between the mobile and fixed base: the Euler vector and Euler angles. These relations are extremely important for the subsequent resolution of static equilibrium equations and transformation matrices. Equation (3) and (4) represents the methods quoted above.

$$FT^S = \begin{bmatrix} \frac{v_2^2 + v_3 v_1^2 \cos \varphi}{v_1^2 + v_2^2} + \frac{(v_3 - 1)v_1 v_2 \sin \varphi}{v_1^2 + v_2^2} & \frac{(v_3 - 1)v_1 v_2 \cos \varphi}{v_1^2 + v_2^2} + \frac{(v_2^2 + v_3 v_1^2) \sin \varphi}{v_1^2 + v_2^2} v_1 \\ \frac{(v_3 - 1)v_1 v_2 \cos \varphi}{v_1^2 + v_2^2} + \frac{(v_1^2 + v_3 v_2^2) \sin \varphi}{v_1^2 + v_2^2} & \frac{(v_1^2 + v_3 v_2^2) \cos \varphi}{v_1^2 + v_2^2} + \frac{(v_3 - 1)v_1 v_2 \sin \varphi}{v_1^2 + v_2^2} v_2 \\ -v_1 \cos \varphi - v_2 \sin \varphi & v_1 \sin \varphi - v_2 \cos \varphi v_3 \end{bmatrix} \quad (3)$$

$$FT^S = \begin{bmatrix} \cos \phi_z \cos \phi_y & -\sin \phi_z \cos \phi_y & \sin \phi_y \\ \sin \phi_x \sin \phi_y \cos \phi_z + \cos \phi_x \sin \phi_z & \cos \phi_x \cos \phi_z - \sin \phi_x \sin \phi_y \sin \phi_z & -\sin \phi_z \cos \phi_y \\ \sin \phi_x \sin \phi_z - \cos \phi_x \sin \phi_y \cos \phi_z & \cos \phi_x \sin \phi_y \sin \phi_z + \sin \phi_x \cos \phi_z & \cos \phi_z \cos \phi_y \end{bmatrix} \quad (4)$$

By performing a polynomial expansion of the trigonometric functions of Eq. (4) and equating to Eq. (3), we find relationships that can be mathematically manipulated and truncated to the third order in order to obtain relations between  $\{\varphi(s), x'(s), y'(s)\}$  e  $\{\phi_x(s), \phi_y(s), \phi_z(s)\}$  in Eqs. (5), (6) and (7):

$$\varphi(s) = \phi_z(s) + \frac{1}{2} \phi_x(s) \phi_y(s) - \frac{1}{6} \phi_z^3(s) \quad (5)$$

$$v_1 = \frac{x'(s)}{r'(s)} = \phi_y(s) - \frac{1}{6} \phi_z^3(s) \quad (6)$$

$$v_2 = -\phi_x(s) + \frac{1}{2} \phi_x(s) \phi_y^2(s) - \frac{1}{6} \phi_x^3(s) \quad (7)$$

Analogously in Eqs. (8), (9) and (10):

$$\phi_x(s, t) = -v_2(s, t) + \frac{1}{2}\varphi(s, t)v_1(s, t) - \frac{1}{6}(v_1^2(s, t) + v_2^2(s, t)) - \frac{1}{2}\varphi^2(s, t)v_2(s, t) \quad (8)$$

$$\phi_y(s, t) = -v_1(s, t) + \frac{1}{2}\varphi(s, t)v_2(s, t) + \frac{1}{6}(v_1^2(s, t) + v_2^2(s, t)) - \frac{1}{2}\varphi^2(s, t)v_1(s, t) \quad (9)$$

$$\phi_z(s, t) = \varphi(s, t) - \frac{1}{12}(v_1^2(s, t) + v_2^2(s, t))\varphi(s, t) \quad (10)$$

The local dynamic behavior of a Cosserat beam element with density  $\rho(s)$  and cross-sectional area  $A(s)$ , as deduced in Antman (1995) is given by the partial differential equations below, Eq. (11) and Eq. (12) respectively:

$$\rho(s)A(s)\frac{\partial^2 \mathbf{r}(s, t)}{\partial t^2} = \frac{\partial \mathbf{n}(s, t)}{\partial s} + \mathbf{f}(s, t) \quad (11)$$

$$\frac{\partial \mathbf{h}(s, t)}{\partial t} = \frac{\partial \mathbf{m}(s, t)}{\partial s} + \mathbf{v}(s, t) \times \mathbf{n}(s, t) + \mathbf{l}(s, t) \quad (12)$$

Where  $n$  is a contact force,  $m$  is the resulting contact moment,  $h$  is an angular momentum,  $f$  is an external force density and  $l$  is an external momentum density.

When using the finite element method, one of the difficulties encountered is to choose the shape functions. These are the ones in charge of indicating the field of displacements within the element from the nodal displacements. They are usually approximated by the use of low order polynomials. In contrast, in Cosserat beam theory, functions can be acquired according to differential equations of static equilibrium and consider nonlinearities of the system. However, for static equilibrium, the equations of motion become ordinary differential equations, where  $s$  is the only independent variable. In the literature, static equilibrium is obtained in the absence of external forces and gravity and Eq. (11), the contact forces must therefore satisfy the condition set forth in Eq. (13):

$$\frac{\partial \mathbf{n}(s)}{\partial s} = 0 \quad (13)$$

And from Eq. (12) the moments of contact satisfy Eq. (13):

$$\frac{\partial \mathbf{m}(s)}{\partial s} + \mathbf{v}(s) \times \mathbf{n}(s) = 0 \quad (14)$$

Once the quantities of the major vectors involved in Eq. (13) and Eq. (14) have been defined, as described by Borges (2010), it is necessary to obtain  $m(s)$  e  $n(s)$  in terms of  $u(s)$ . The constructive relations of the material can help in obtaining these. It should be noted that in this work, a constitutive model was used, where the characteristics of a linear elastic material were adopted, based on the constitutive relations of Kirchhoff (Cao et al., 2005). Thus, it is assumed that the Young's modulus ( $E$ ), the shear modulus ( $G$ ) and the specific mass along the Cosserat beam element are only function of the spatial variable  $s$ , and the center of mass coincides with the cross-sectional centroid.

Therefore, the use of these relationships, forces and contact torque are given as functions of linear and angular deformations, respectively (Borges, 2010) and, as a result, Eq. (13) and Eq. (14) can be written in terms of the forces and moments of contact in the form of a highly non-linear system, given by the Eq. (15), (16), (17) and (18):

$$n'_1(s) = u_3(s)n_2(s) - u_2(s)n_3(s) \quad (15)$$

$$n'_2(s) = u_1(s)n_3(s) - u_3(s)n_1(s) \quad (16)$$

$$n'_3(s) = u_2(s)n_1(s) - u_1(s)n_2(s) \quad (17)$$

$$m'_3(s) = u_2(s)m_1(s) - u_1(s)m_2(s) \quad (18)$$

To find the form functions it becomes necessary to solve the above highly non-linear system which comprises from Eq. (15) to Eq. (18). Note that this equation can not be developed through direct integration. Therefore, the perturbation method is used to obtain the approximate solution (Nayfeh, 1985). For this purpose, a perturbation method oriented to this type of solution was used and, among the various available methods, the method of Frobenius (Arfken et al., 2000) was chosen.

In order to simplify the form functions, it was adopted to truncate them in the third order. The generic displacements of the Cosserat beam, for  $s = [0, L]$  are, according to the Frobenius method found in Eqs. (19), (20), (21) and (22).

$$x(s) = \bar{x}(\bar{s})L = \varepsilon x_1(s) + \varepsilon^2 x_2(s) + \varepsilon^3 x_3(s) \quad (19)$$

$$y(s) = \bar{y}(\bar{s})L = \varepsilon y_1(s) + \varepsilon^2 y_2(s) + \varepsilon^3 y_3(s) \quad (20)$$

$$z(s) = \bar{z}(\bar{s})L = \varepsilon z_1(s) + \varepsilon^2 z_2(s) + \varepsilon^3 z_3(s) \quad (21)$$

$$\varphi(s) = \bar{\varphi}(\bar{s})L = \varepsilon \varphi_1(s) + \varepsilon^2 \varphi_2(s) + \varepsilon^3 \varphi_3(s) \quad (22)$$

It should be emphasized that these functions can be approximated to the order required by the user, but the computational costs are dramatically increased for higher orders.

Equation (23) was obtained using symbolic manipulation software. Due to the complexity of their individual terms, they were intentionally omitted. From the development of the formulation and after several mathematical manipulations, we find the ordinary differential equation of motion with nonlinearities of the same order of displacement functions (third order) for static analysis.

$$K^{(e)} q^{(e)}(t) + g^{(e)}(q^{(e)}(t)) = f^{i(e)}(t) + f^{c(e)}(t) + f^{d(e)}(t, q^{(e)}) \quad (23)$$

Where,  $K^{(e)}$  is the linear stiffness matrix,  $g^{(e)}(q^{(e)}(t))$  is a non-linear vector with quadratic and cubic terms on the components of  $q^{(e)}$ ,  $q^{(e)}$  is the nodal displacement vector,  $f^{i(e)}$  represents the internal forces and the momentum,  $f^{c(e)}$  the external forces and impulse e  $f^{d(e)}$  from the elements of distributed load.

The boundary conditions are imposed, and the global matrices and global forces vectors are assembled from the elementary matrices and the elementary vectors, according to the classical finite element theory. For more details on this implementation and construction of global matrices, the reader can refer to the work of Cao et al. (2005) and Borges (2010).

### 3. RESULTS

For the numerical calculation, the Matlab® computer program was used. The program, from the definition of initial conditions, simulates the field of stresses and displacements. To validate this, a comparison of results from its use will be presented below in two cases addressed in the literature.

#### 3.1 Case 1 - Cantilever beam loaded by a transverse force

The first case consists of the application of a force at the free end of a free-set beam studied by Yilmaz (2016). The geometric properties of the structure are set out in Tab. 1.

Table 1. Properties of the beam.

Property	Values
Young's Module	207[Gpa]
Length	2 [m]
Width of Cross Section	0,1 [m]
Height of Cross Section	0,1[m]

The load applied at the free end is equivalent to  $P = 3EI / L^2 = 1293.75$  kN, that is, the displacement, if calculated by the linear theory using the maximum arrow approach, results in a value equivalent to the length of the beam, in case 2 m. The application of force is expressed in Fig. 2, and shear stresses were disregarded.

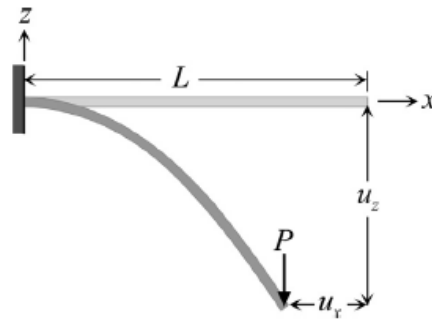


Figure 2. Beam loaded by a transverse force (case 1) (YILMAZ, 2016)

In addition, Yilmaz (2016) presented different results taking into account the variation of the number of elements used in the simulation and compared its response with the studies of Jonkera and Meijaard (2013) and Gerstmayr and Irschik (2008).

The present simulation also considered the discretization of the structure with different numbers of elements, where the number of nodes is equivalent to the number of elements plus one, and each node covers 6 degrees of freedom. Table 2 shows the comparison of the free-end displacements for the studied study achieved with the different methodologies mentioned above. Table 2 uses displacement orientation according to Fig. 2. The unit of measurement of displacements is meter.

Table 2. Displacement Comparison (case 1).

Number of Elements	Present		Yilmaz and Omurtag		Jonkera and Meijaard		Gerstmayr and Irschik	
	$u_x$	$u_z$	$u_x$	$u_z$	$u_x$	$u_z$	$u_x$	$u_z$
1	<b>0.358761</b>	<b>1.054525</b>	0.355272	1.126280	0.901067	1.521304	0.362245	0.994145
2	<b>0.490001</b>	<b>1.187340</b>	0.458556	1.184997	0.574104	1.276622	0.488926	1.175223
4	<b>0.503357</b>	<b>1.204262</b>	0.495015	1.201768	0.523295	1.223753	0.507429	1.205534
8	<b>0.508123</b>	<b>1.207150</b>	0.505084	1.205886	0.512121	1.211296	0.508509	1.207198
16	<b>0.50854</b>	<b>1.207239</b>	0.507669	1.206903	0.509427	1.208249	0.508537	1.207239
32	<b>0.508537</b>	<b>1.207241</b>	0.508320	1.207156	0.508759	1.207492	0.508537	1.207240
64	<b>0.508537</b>	<b>1.207240</b>	0.508483	1.207219	0.508593	1.207303	0.508537	1.207240
128	<b>0.508537</b>	<b>1.207240</b>	0.508524	1.207235	0.508551	1.207256	0.508537	1.207240

It is noticed that due to the non-linearities considered, due to the large displacements imposed in the system, the structure showed an increase in the stiffness as the displacement increased, resulting in a final displacement smaller than the displacement expected by the linear theory. This increase in stiffness occurs because as the vertical displacement increases a horizontal force (which consequently generates the displacement  $u_x$ ) arises, and the whole thereof generates a resultant force that stiffens the structure.

### 3.2 Case 2 - Cantilever beam loaded by a transverse force with different materials

The second case to validate the methodology was based on the work of Wang (2015). The numerical example considered a set-free rectangular beam of 508 mm in length, 25.4 and 50.8 mm in width and height of the cross section respectively. The beam was divided into four layers consisting of two isotropic materials with different moduli of elasticity. The modulus of elasticity of the upper and lower layers is  $2.6 \times 10^7$  psi and the central layers,  $2.6 \times 10^6$  psi. The Poisson coefficient for both materials is 0.3. Wang (2015) divided the structure into 5 one-dimensional cubic elements along the reference line and into 192 two-dimensional quadrilateral elements in the cross section, each containing 8 nodes. The beam undergoes transverse loads at its free end of magnitude 89 kN. Figure 3 shows the representation of the beam, the layers of different isotropic materials, their discretization and the profile of displacements after application of the force at the free end.

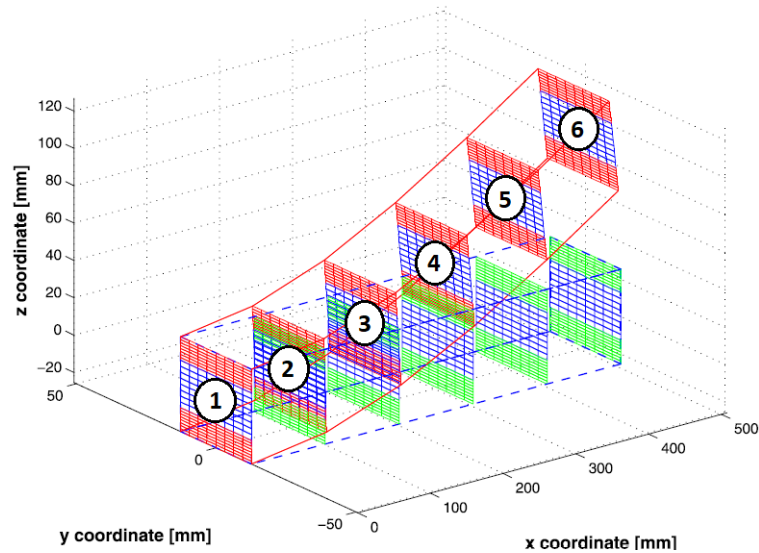


Figure 3. Rectangular beam (case 2) (WANG, 2015).

For the proposed simulation, the same geometric and physical characteristics of the study in question are considered. It is known that in the theory of Cosserat rods the modulus of elasticity ( $E$ ) can be approximated to a constant, so to obtain an average value, it was decided to use the calculation of the mean elastic modulus of Voigt, which assumes an iso-deformation and relates the different modules with the volumetric fractions of each material. The above mentioned fact can be represented in Eq. (24) where,  $E_c$  is the mean modulus of elasticity,  $E_d$  and  $E_m$  are the modules of material 1 and 2 and  $V_d$  and  $V_m$  are the volumetric fractions of material 1 and 2.

$$E_c = E_d V_d + E_m V_m \quad (24)$$

Regarding the discretization of the structure, it was divided into 10 equally spaced beam elements, with 11 nodes and 6 degrees of freedom per node. The force was applied at node 11 as shown in Fig. 4.

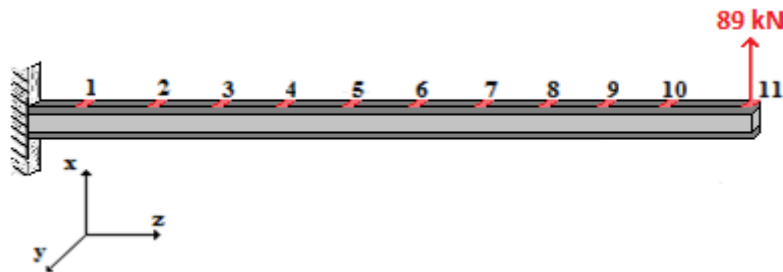


Figure 4. Beam loaded by a transverse force (case 2)

In order to validate the presented case, the displacements for the nodes 1,3,5,7,9 and 11 of the simulated structure are presented in Table 3 and these are compared to the coincident points 1 to 6 (in parentheses) shown in Fig. 3 from the work of Wang (2015). Both displacements are expressed in meters.

Table 3. Displacement Comparison (Case 2)

Node	Present displacement (m)	Wang displacement (m)	Error (%)
1 (1)	0	0	0
3 (2)	0.0045	0.006	25
5 (3)	0.028	0.032	12,5
7 (4)	0.0401	0.043	6,9
9 (5)	0.0620	0.063	1,6
11(6)	0.0896	0.090	0,4

Table 3 shows that the displacement profile presents a smaller error as the imposed displacement increases, due to the theory of Cosserat beams being a theory that presents greater precision for displacements characterized in the nonlinear regime. It should be emphasized that for displacements greater than 1% of beam length (limit value for linear regime), the numerical procedure presented was effective with a maximum error of 2%.

#### 4. CONCLUSION

It can be noted from the comparison evaluation that the results were satisfactory, since they present a small variation between the results of other authors for the cases studied and the presented procedure. For the first case, the displacement exhibited greater precision with the structure being divided into fewer elements, whereas for other methods of the literature, the results converge with the division of the structure into more elements. Already for the second case, the methodology proved to be effective for beams with the presence of different materials presenting greater precision in larger displacements.

#### 5. ACKNOWLEDGEMENTS

The authors are grateful to the Federal Technological University of Paraná (Cornélio Procópio) and the Araucária Foundation for material and financial support.

#### REFERENCES

- Arfken, G.;Weber, H. J.; Harris, F., 2000, *Mathematical Methods for Physicists*. 5.ed. Academic Press Inc., San Fiego. 1112p.
- Antman, S.S, 1995, “Nonlinear Problems of Elasticity”. *Applied Mathematical Sciences* 107, New York: Springer-Verlag.
- Bathe, K. J. *Conserving Energy And Momentum In Nonlinear Dynamics: A Simple Implicit Time Integration Scheme*. *Computers and Structures*. v.85, p. 437–445. 2007.
- Borges, A.S., 2010, “Desenvolvimento de procedimentos de modelagem de interação fluido-estrutura combinado a teoria de vigas de cosserat e a metodologia de fronteira imersa”, Tese de Doutorado, Universidade Federal de Uberlândia, Uberlândia.
- Cao, D.Q., Dongsheng, L., Charles, H., Wang, T., “Three dimensional nonlinear dynamics of slender structures: Cosserat rod element approach”, *International Journal of Solids and Structures*.
- Fish, J., Belytschko, T. *Um Primeiro Curso de Elementos Finitos*. Rio de Janeiro. LTC – Livros Técnicos e Científicos,2009.
- Gerstmayr J, Irschik H. On the correct representation of bending and axial deformation in the absolute nodal coordinate formulation with an elastic line approach. *J Sound Vib* 2008;318:461–87.
- Jonker JB, Meijaard JP. A geometrically non-linear formulation of a threedimensional beam element for solving large deflection multibody system problems. *Int J Non-Linear Mech* 2013;53:63–74.
- Nayfeh, A.H., 1985, “Problems in Perturbation”, Wiley, New York.
- Wang, Jielong (2015). Implementation of geometrically exact beam element for nonlinear dynamics modeling. *Multibody System Dynamics*, 35(4), 377-392. doi:10.1007/s11044-015-9457-8
- Yilmaz, Murat & Omurtag, Mehmet. (2016). Large deflection of 3D curved rods: An objective formulation with principal axes transformations. *Computers & Structures*. 163. 71-82. 10.1016/j.compstruc.2015.10.010.

#### 6. RESPONSIBILITY NOTICE

“The authors are the only responsible for the printed material included in this paper”.